Transition-metal Schiff-base Complexes as Ligands in Tin Chemistry. Part 5.† Structural Studies of Intimate Ion-paired Heterobimetallic Complexes of Tin(IV) and Nickel, Copper or Zinc with 3-Methoxysalicylaldimine Ligands‡

Brenda Clarke, Demond Cunningham,* John F. Gallagher, Tim Higgins, Patrick McArdle, John McGinley, Máire Ní Cholchúin and David Sheerin
Chemistry Department, University College, Galway, Ireland

1 : 1 Adducts have been formed between $SnMe_2(NCS)_2$ and $SnBu^n_2(NCS)_2$ with [Ni(3MeO-salpd)]·H_2O [3MeO-H_2salpd = *N,N'*-bis(3-methoxysalicylidene)propane-1,3-diamine] and [Ni(3MeO-salbn)]·H_2O [3MeO-H_2salbn = *N,N'*-bis(3-methoxysalicylidene)butane-1,4-diamine] and are best represented as the intimate ion-paired adducts $[SnR_2]^{2+}\cdot[NiL(NCS)_2]^{2-}$ [L = Schiff-base ligand; R = Me or Bu^n] in each of which the tin atom sits in the plane of, and is held by donor bonds from, the four Schiff-base oxygen atoms. A crystal-structure determination of $[SnMe_2]^{2+}\cdot[Ni(3MeO\text{-}salpd)(NCS)_2]^{2-}$ revealed a tin co-ordination geometry which can be described as skew trapezoidal bipyramidal. The large unoccupied volume of the tin co-ordination sphere results in tin readily increasing its co-ordination number to seven, as demonstrated crystallographically in $[SnMe_2\cdot dmf]^{2+}\cdot[Ni(3MeO\text{-}salpd)(NCS)_2]^{2+}$ (dmf = dimethylformamide), which contains tin in a pentagonal-bipyramidal co-ordination environment with *trans* methyl groups and five donor oxygen atoms in the equatorial plane. X-Ray structural studies of both $[SnBu^n_2]^{2+}\cdot[Ni(3MeO\text{-}salpd)(NCS)_2]^{2-}$ and $[SnBu^n_2]^{2+}\cdot[Ni(3MeO\text{-}salbn)(NCS)_2]^{2-}$ revealed the presence of molecular association resulting from weak intermolecular thiocyanate contacts, thus providing each tin with pseudo-pentagonal-bipyramidal co-ordination geometry. These latter adducts readily formed tin donor bonds with dmf. The 1 : 1 adduct formed between $SnPh_2(NCS)_2$ and [Ni(3MeO-salpd)]·H_2O was shown, from an X-ray crystallographic study, to be the intimate ion-paired heterobimetallic complex $[SnPh_2(NCS)]^+\cdot[Ni(3MeO\text{-}salpd)(NCS)(MeCN)]^-$ in which tin has pentagonal-bipyramidal geometry with *trans* phenyl groups. Infrared and tin-119 Mössbauer spectroscopic data clearly demonstrate that a similar pentagonal-bipyramidal co-ordination geometry exists about tin in the complexes $[SnR_2(NCS)]^+\cdot[ML(NCS)]^-\cdot nH_2O$ (R = Me or Bu^n; M = Cu or Zn; *n* = 0, 1 or 2).

The ability of metal salicylaldimine complexes to act as effective bidentate donor ligands to tin(IV) halides, organotin(IV) halides and pseudo-halides, and tin(II) halides is well documented[1-7] and crystallographic data have confirmed the donor role of the phenolic oxygens in the structures of $SnMe_2Cl_2\cdot$[Ni(salen)] and $SnBu^nCl_2(OMe)\cdot$[CoCl(salen)] [H_2salen = *N,N'*-bis(salicylidene)ethane-1,2-diamine].[8,9] Studies in this laboratory have demonstrated that when there are methoxy substituents *ortho* to the phenolic oxygens in the metal salicylaldimine complexes, *i.e.* 3-methoxysalicylaldimine complexes, their complexing role towards tin Lewis acids is markedly altered. In Part 3 of this series it was shown that when the imine nitrogen bridging group is a two carbon-atom bridge the metal Schiff-base complexes form 1 : 1 addition complexes with diorganotin(IV) halides which, in fact, were shown to be monoaqua adducts of the diorganotin(IV) halide Lewis acids with the donor water in each case being hydrogen bonded to the salicylaldimine oxygen atoms.[6] In no case did it appear that the phenolic oxygens were forming donor bonds to tin. It was also demonstrated that triphenyltin(IV) chloride forms a similar type aqua adduct with [Ni(3MeO-salpd)]·H_2O [3MeO-H_2salpd = *N,N'*-bis(3-methoxysalicylidene)propane-1,3-diamine].[7] Since all of the diorganotin(IV) chloride and thiocyanate adducts with [Ni(3MeO-salen)]·H_2O [3MeO-H_2salen = *N,N'*-bis(3-methoxysalicylidene)ethane-1,2-diamine], [Ni(3MeO-salpn)]·H_2O [3MeO-H_2salpn = *N,N'*-bis(3-methoxysalicylidene)propane-1,2-diamine] and [Ni(3MeO-salphen)]·H_2O [3MeO-H_2salphen = *N,N'*-bis(3-methoxysalicylidene)-*o*-phenylenediamine] were brick-red and diamagnetic, it was surprising to find that the reactions of diorganotin(IV) thiocyanates with [Ni(3MeO-salpd)]·H_2O and [Ni(3MeO-salbn)]·H_2O [3MeO-H_2salbn = *N,N'*-bis(3-methoxysalicylidene)butane-1,4-diamine] led to the isolation of blue or purple paramagnetic 1 : 1 addition complexes. The present paper describes crystallographic and tin-119 Mössbauer spectroscopic studies which identify these paramagnetic adducts as an interesting class of intimate ion-paired heterobimetallic complexes.

Experimental

Infrared spectra were recorded on a Perkin-Elmer 983G spectrometer. Details of the Mössbauer spectrometer and spectrum curve-fitting procedure have been published.[4]

Synthesis and Crystallisation of the Adducts.—All of the 1 : 1 bimetallic adducts of Table 1 were prepared by stirring the organotin Lewis acid (0.01 mol) and the metal Schiff-base complex (0.01 mol) in acetonitrile (chloroform was found to be equally satisfactory) for several hours. The air-stable blue or purple nickel–tin adducts, green copper–tin adducts and pale yellow zinc–tin adducts were isolated by filtration and dried under vacuum. The complexes all had low solubilities in common organic solvents but readily dissolved in pyridine, dimethylformamide (dmf) or dimethyl sulfoxide. The dmf adducts of Table 1 were readily obtained by stirring the parent bimetallic complexes in dmf. The dmf adducts readily precipitated from solution at room temperature.

† Part 4 is ref. 7.
‡ *Supplementary data available:* see Instructions for Authors, *J. Chem. Soc., Dalton Trans.*, 1994, Issue 1, pp. xxiii–xxviii.

With the exception of $[SnMe_2{\cdot}dmf]^{2+}{\cdot}[Ni(3MeO\text{-}salpd)(NCS)_2]^{2-}$, crystals of the nickel–tin complexes were grown from hot saturated acetonitrile solutions which were allowed to cool slowly over a period of approximately 15 h. Acetonitrile solutions of $[SnBu^n_2]^{2+}{\cdot}[Ni(3MeO\text{-}salbn)(NCS)_2]^{2-}$ yielded not only blue crystals of the bimetallic adduct but also green crystals of $Ni[Ni(3MeO\text{-}salbn)(NCS)]_2$, the structure of which will be described elsewhere. Relatively dilute greenish blue dmf solutions of $[SnMe_2]^{2+}{\cdot}[Ni(3MeO\text{-}salpd)(NCS)_2]^{2-}$, prepared at room temperature, yielded pale blue crystals of $[SnMe_2{\cdot}dmf]^{2+}{\cdot}[Ni(3MeO\text{-}salpd)(NCS)_2]^{2-}$ after several hours. These crystals had very low solubility in dmf.

X-Ray Crystallography.—Crystallographic details are in Table 2. All five structures were solved by direct methods, SHELX 86,[10] and refined by full-matrix least squares, SHELXL 93.[11] Data were corrected for Lorentz and polarisation effects but not for absorption. Hydrogen atoms were included in calculated positions for final refinement cycles. All non-hydrogen atoms were refined anisotropically, except in the case (discussed later) of certain carbon atoms of **C**. In the cases of **A**, **D** and **E** the central atom of the propylene bridge showed disorder over two positions having site occupancies of 50%. In **A** these positions were related by the two-fold axis. In **B** there is a clear suggestion from bond length and angle data and

Table 1 Analytical data (%) *

Complex	C	N	H
$[SnMe_2]^{2+}{\cdot}[Ni(3MeO\text{-}salpd)(NCS)_2]^{2-}$	40.55 (41.50)	8.60 (8.40)	3.85 (3.90)
$[SnMe_2{\cdot}dmf]^{2+}{\cdot}[Ni(3MeO\text{-}salpd)(NCS)_2]^{2-}$	42.55 (42.25)	9.65 (9.50)	4.40 (4.45)
$[SnBu^n_2]^{2+}{\cdot}[Ni(3MeO\text{-}salpd)(NCS)_2]^{2-}$	46.50 (46.75)	7.55 (7.50)	5.15 (5.10)
$[SnBu^n_2{\cdot}dmf]^{2+}{\cdot}[Ni(3MeO\text{-}salpd)(NCS)_2]^{2-}$	47.35 (46.95)	8.85 (8.55)	5.15 (5.50)
$[SnMe_2]^{2+}{\cdot}[Ni(3MeO\text{-}salbn)(NCS)_2]^{2-}$	41.95 (42.40)	7.80 (8.25)	4.50 (4.10)
$[SnMe_2{\cdot}dmf]^{2+}{\cdot}[Ni(3MeO\text{-}salbn)(NCS)_2]^{2-}$	43.60 (43.05)	9.45 (9.30)	4.45 (4.65)
$[SnBu^n_2]^{2+}{\cdot}[Ni(3MeO\text{-}salbn)(NCS)_2]^{2-}$	47.60 (47.45)	7.50 (7.40)	5.50 (5.25)
$[SnBu^n_2{\cdot}dmf]^{2+}{\cdot}[Ni(3MeO\text{-}salbn)(NCS)_2]^{2-}$	47.35 (47.60)	8.65 (8.40)	5.35 (5.65)
$[SnPh_2(NCS)]^{+}{\cdot}[Ni(3MeO\text{-}salpd)(NCS)(MeCN)]^{-}$	50.45 (50.45)	8.10 (8.45)	4.15 (4.00)
$[SnMe_2(NCS)]^{+}{\cdot}[Cu(3MeO\text{-}salpd)(NCS)]^{-}$	41.00 (41.30)	8.40 (8.40)	3.90 (3.90)
$[SnMe_2(NCS)]^{+}{\cdot}[Cu(3MeO\text{-}salpd)(NCS)]^{-}{\cdot}2H_2O$	39.25 (39.15)	8.05 (7.75)	4.05 (4.25)
$[SnBu^n_2(NCS)]^{+}{\cdot}[Cu(3MeO\text{-}salpd)(NCS)]^{-}{\cdot}H_2O$	45.60 (45.20)	7.45 (7.25)	5.00 (5.20)
$[SnMe_2]^{2+}{\cdot}[Cu(3MeO\text{-}salbn)(NCS)_2]^{2-}{\cdot}H_2O$	40.35 (40.90)	8.30 (7.95)	4.05 (4.25)
$[SnBu^n_2(NCS)]^{+}{\cdot}[Zn(3MeO\text{-}salpd)(NCS)]^{-}$	46.40 (46.15)	7.80 (7.45)	5.20 (5.05)

* Theoretical data are in parentheses.

Table 2 Crystallographic data *

	A	B	C	D	E
Empirical formula	$C_{23}H_{26}N_4NiO_4S_2Sn$	$C_{29}H_{38}N_4NiO_4S_2Sn$	$C_{30}H_{40}N_4NiO_4S_2Sn$	$C_{26}H_{27}N_5NiO_5S_2Sn$	$C_{35}H_{33}N_5NiO_4S_2Sn$
M	664	748.15	762.18	731.05	829.18
Crystal system	Monoclinic	Monoclinic	Monoclinic	Monoclinic	Triclinic
Space group	$C2/c$	$P2_1/c$	$P2_1/c$	$P2_1/n$	$P\bar{1}$
a/Å	14.907(2)	11.755(2)	12.194(2)	13.3997(12)	9.4579(11)
b/Å	11.588(2)	20.462(5)	20.305(4)	11.8640(14)	10.560(2)
c/Å	16.286(2)	14.256(4)	14.366(4)	19.917(2)	19.514(3)
α/°	90	90	90	90	96.080(13)
β/°	112.808(10)	103.83(2)	104.34(2)	103.805(8)	96.998(11)
γ/°	90	90	90	90	113.485(12)
U/Å^3	2593.3(6)	3329.5(13)	3446.2(13)	3074.2(6)	1748.5(5)
Z	4	4	4	4	2
D_c/Mg m^{-3}	1.701	1.493	1.469	1.580	1.575
Absorption coefficient/mm^{-1}	1.887	1.479	1.430	1.603	1.418
F(000)	1336	1528	1560	1472	840
Crystal size/mm	0.35 × 0.32 × 0.25	0.30 × 0.27 × 0.25	0.25 × 0.25 × 0.20	0.34 × 0.2 × 0.24	0.25 × 0.10 × 0.08
θ Range/°	2.30–23.97	2.04–23.95	2.01–23.97	2.01–31.96	2.13–23.97
Index ranges	$0 \leqslant h \leqslant 15$, $0 \leqslant k \leqslant 12$, $-17 \leqslant l \leqslant 17$	$0 \leqslant h \leqslant 12$, $0 \leqslant k \leqslant 21$, $-15 \leqslant l \leqslant 15$	$0 \leqslant h \leqslant 12$, $0 \leqslant k \leqslant 20$, $-14 \leqslant l \leqslant 14$	$-14 \leqslant h \leqslant 14$, $0 \leqslant k \leqslant 12$, $0 \leqslant l \leqslant 20$	$0 \leqslant h \leqslant 10$, $-11 \leqslant k \leqslant 11$, $-20 \leqslant l \leqslant 20$
Reflections collected	2098	5509	5439	7389	5936
Independent reflections (R_{int})	1986 (0.0336)	5101 (0.0254)	5113 (0.0353)	6976 (0.0127)	5399 (0.0118)
Data, restraints, parameters	1985, 0, 159	5100, 0, 370	5113, 0, 359	6976, 0, 370	5392, 0, 433
Goodness-of-fit on F^2	0.851	0.963	1.180	1.067	1.011
Final R indices ($I > 2\sigma I$)					
R	0.0381	0.0383	0.0511	0.0381	0.0267
R'	0.0961	0.1045	0.1511	0.1142	0.0669
Final R indices (all data)					
R	0.0459	0.0577	0.0670	0.0494	0.0456
R'	0.1034	0.111 50	0.1603	0.1200	0.0718
Largest difference peak, hole/e Å^{-3}	1.030, −1.299	1.560, −0.837	1.101, −1.102	0.774, −0.768	0.455, −0.409

* Details in common: T/K 293(2); λ(Mo-Kα) 0.710 69 Å; refinement, full-matrix least squares on F^2; $R = (\Sigma||F_o| - |F_c||)/\Sigma|F_o|$ (based on F); $R' = [\Sigma w(|F_o| - |F_c|)^2/\Sigma w(|F_o|)^2]^{\frac{1}{2}}$ (based on F^2); $w = q/[(\sigma F_o)^2 + (a^*P)^2 + b^*P + d + e^*\sin(\theta)]$; goodness-of-fit $= [\Sigma w(|F_o^2| - |F_c^2|)^2/(N_{obs} = N_{parameters})]^{\frac{1}{2}}$.

U values that the refined position for the central atom of the propylene bridge is, in reality, the average of disordered positions. However, peaks corresponding to these positions could not be detected. In the case of **C**, in which complex disorder of the four carbon atoms of the nitrogen bridging group occurred, all efforts to model the disorder in a realistic manner were unsuccessful. Ultimately, the four major peaks, which, in fact, corresponded to the most realistic carbon positions, were refined isotropically. In **A** and **D** the highest peaks in the final difference maps were within 1 Å from tin. In the case of **C** the highest peaks in the final difference map were close to the carbon atoms of the imine nitrogen bridging group, these being the carbon atoms which created problems (as described above) during structure refinement. In **B** the highest peaks in the final difference map were close to S(2) and C(13), and in **E** they were close to S(1) and S(2); S(2) and C(13) (of structure **B**) and S(1) and S(2) (of structure **E**) were the atoms which refined least satisfactorily. Calculations were carried out on a VAX 6610 computer. Final atomic coordinates are in Tables 3–7. The program ORTEP[12] was used to produce the drawings in Figs. 1–3, 6 and 7 and PLUTO[13] to produce the drawing in Fig. 5.

Additional material available from the Cambridge Crystallographic Data Centre comprises H-atom coordinates, thermal parameters and remaining bond lengths and angles.

Table 3 Fractional atomic coordinates (× 10^4) for complex **A**

Atom	*x*	*y*	*z*
Sn	0	1142(1)	2500
Ni	0	3955(1)	2500
S(1)	−2128(1)	2895(1)	3868(1)
O(1)	525(2)	2555(2)	3325(2)
O(2)	946(2)	578(3)	4124(2)
N(1)	−1232(3)	3859(3)	2818(3)
N(2)	575(2)	5054(3)	3522(2)
C(1)	−1596(3)	3464(4)	3257(3)
C(2)	397(6)	6623(8)	2455(6)
C(3)	486(4)	6314(4)	3337(3)
C(4)	928(3)	4755(4)	4336(3)
C(5)	1100(3)	3603(4)	4704(3)
C(6)	1519(3)	3532(5)	5644(3)
C(7)	1754(4)	2498(4)	6076(3)
C(8)	1590(3)	1480(5)	5592(3)
C(9)	1159(3)	1523(4)	4681(3)
C(10)	916(3)	2569(3)	4224(3)
C(11)	1096(4)	−546(4)	4518(4)
C(12)	−1192(3)	455(4)	2714(3)

Discussion

The striking similarities in the structures of $[SnMe_2]^{2+}$·[Ni(3MeO-salpd)$(NCS)_2$]$^{2-}$ **A**, its dibutyltin analogue **B** and $[SnBu^n_2]^{2+}$·[Ni(3MeO-salbn)$(NCS)_2$]$^{2-}$ **C** are clearly demonstrated by the asymmetric units of Figs. 1–3 respectively and the bonding parameters of Tables 8–10 respectively. In fact, **B** and **C**, crystallising in the same space group with very similar cell parameters (see Table 2) and with similar cell packing (see Fig. 6), can be considered as a pseudo isomorphic pair. The main structural difference between the complexes is that the structures of the dibutyltin complexes, **B** and **C**, display intermolecular interactions which are absent in the structure of the dimethyltin complex **A**, and for this reason the latter structure is discussed first.

Perhaps the most significant revelation of the crystallographic study of complex **A** is that the thiocyanate groups have migrated from tin to nickel which, as a result, attains six-coordination (thus accounting for the paramagnetic nature and blue colour of the complex). The dimethyltin cation is located with the tin atom in the plane of, and engaged in donor-bond formation with, the four Schiff-base oxygen atoms. The tin and oxygen atoms are almost co-planar. The oxygen atoms are arranged at the corners of a regular trapezium such that the lines joining the phenolic oxygens and the methoxy oxygens define the short and long parallel edges respectively. Tin is much closer to the phenolic than the methoxy oxygen atoms such as to give extremely unequal Sn–O bond lengths, those involving the phenolic oxygens being 2.069(3) Å and those involving the methoxy oxygens 2.554(3) Å. The methyl groups bonded to tin fall away symmetrically from their true *trans* locations, towards the methoxy atoms, thus providing a C–Sn–C bond angle of 135.3(3)°. The geometry about tin is most aptly described as skew trapezoidal bipyramidal.

The very short bonds from tin to the phenolic oxygens contrast sharply with the much longer corresponding bond lengths of 2.40(1) and 2.56(1) Å observed for $SnMe_2Cl_2$·[Ni(salen)],[8] and 2.410(6) and 2.300(6) Å for $SnBu^nCl_2$(OMe)·[CoCl(salen)],[9] this latter complex almost certainly containing a stronger tin Lewis acid that that in **A**. In view of the very short Sn–O bond lengths of complex **A**, two chemical representations of its structure, as depicted in Fig. 4 can be considered.

Table 4 Fractional atomic coordinates (× 10^4) for complex **B**

Atom	*x*	*y*	*z*	Atom	*x*	*y*	*z*
Sn	1731(1)	1495(1)	2258(1)	C(10)	−91(4)	−313(3)	2744(4)
Ni	2286(1)	437(1)	4040(1)	C(11)	480(5)	−561(3)	3693(4)
S(1)	3698(2)	−791(1)	1689(1)	C(12)	1754(6)	−705(4)	5204(5)
S(2)	638(3)	2229(1)	5367(2)	C(13)	2621(10)	−443(5)	5885(7)
O(1)	1095(3)	639(2)	2759(2)	C(14)	3634(5)	−110(3)	5955(4)
O(2)	2942(3)	1268(2)	3546(2)	C(15)	4338(4)	879(3)	5487(4)
O(3)	−26(3)	977(2)	1016(2)	C(16)	4503(4)	1463(3)	4948(4)
O(4)	3307(3)	2379(2)	2768(3)	C(17)	5432(5)	1868(3)	5393(4)
N(1)	1363(4)	−340(2)	4298(3)	C(18)	5677(6)	2431(3)	4965(5)
N(2)	3590(4)	421(2)	5252(3)	C(19)	4988(5)	2618(3)	4081(5)
N(3)	3125(4)	−136(2)	3218(3)	C(20)	4064(5)	2232(2)	3637(4)
N(4)	1380(4)	1080(3)	4738(4)	C(21)	3816(4)	1644(2)	4045(4)
C(1)	3344(4)	−412(3)	2578(4)	C(22)	2630(5)	1186(3)	1206(4)
C(2)	1125(5)	1557(3)	4997(4)	C(23)	3942(5)	1148(3)	1540(4)
C(3)	−606(6)	1169(3)	56(4)	C(24)	4504(5)	905(3)	755(4)
C(4)	3523(7)	2953(3)	2269(5)	C(25)	5795(6)	809(4)	1074(5)
C(5)	215(4)	253(2)	2306(3)	C(26)	617(5)	2202(3)	2635(4)
C(6)	−420(4)	424(2)	1379(4)	C(27)	−629(5)	2017(3)	2555(5)
C(7)	−1363(5)	56(3)	893(4)	C(28)	−1366(7)	2581(5)	2779(6)
C(8)	−1679(6)	−497(3)	1334(5)	C(29)	−2483(10)	2415(6)	2849(9)
C(9)	−1052(5)	−675(3)	2234(5)				

Table 5 Fractional atomic coordinates ($\times 10^4$) for complex **C**

Atom	*x*	*y*	*z*	Atom	*x*	*y*	*z*
Sn	1757(1)	1485(1)	2225(1)	C(10)	−92(6)	−288(3)	2688(5)
Ni	2296(1)	408(1)	4008(1)	C(11)	443(6)	−567(4)	3606(6)
S(1)	3658(3)	−834(1)	1703(2)	C(12)	1706(15)	−853(7)	5023(11)
S(2)	660(3)	2188(1)	5348(2)	C(13)	1917(14)	−599(8)	5814(12)
O(1)	1148(4)	623(2)	2701(3)	C(14)	2959(18)	−302(12)	6250(16)
O(2)	2945(4)	1247(2)	3505(3)	C(15)	3792(6)	−136(3)	5920(5)
O(3)	52(4)	998(2)	979(3)	C(16)	4322(6)	881(4)	5429(5)
O(4)	3261(4)	2375(2)	2704(3)	C(17)	4420(6)	1479(3)	4904(5)
N(1)	1329(6)	−371(4)	4215(5)	C(18)	5311(7)	1907(4)	5349(6)
N(2)	3616(5)	406(3)	5209(4)	C(19)	5520(9)	2464(5)	4916(8)
N(3)	3093(5)	−183(3)	3214(5)	C(20)	4864(8)	2640(4)	4053(7)
N(4)	1433(6)	1062(4)	4657(5)	C(21)	3981(6)	2244(3)	3587(5)
C(1)	3304(6)	−454(4)	2582(6)	C(22)	3757(5)	1653(3)	4002(5)
C(2)	1153(7)	1531(4)	4949(5)	C(23)	2610(6)	1189(4)	1179(5)
C(3)	−480(8)	1181(5)	8(6)	C(24)	3872(6)	1129(4)	1503(5)
C(4)	3478(9)	2946(5)	2195(8)	C(25)	4411(7)	886(4)	713(6)
C(5)	250(5)	267(3)	2260(5)	C(26)	5654(8)	789(6)	1034(7)
C(6)	−379(5)	449(3)	1339(5)	C(27)	698(7)	2209(4)	2618(5)
C(7)	−1338(7)	125(5)	875(6)	C(28)	−519(7)	2052(4)	2480(7)
C(8)	−1681(9)	−410(6)	1297(7)	C(29)	−1200(9)	2596(6)	2746(8)
C(9)	−1072(7)	−614(5)	2171(6)	C(30)	−2329(14)	2487(9)	2648(13)

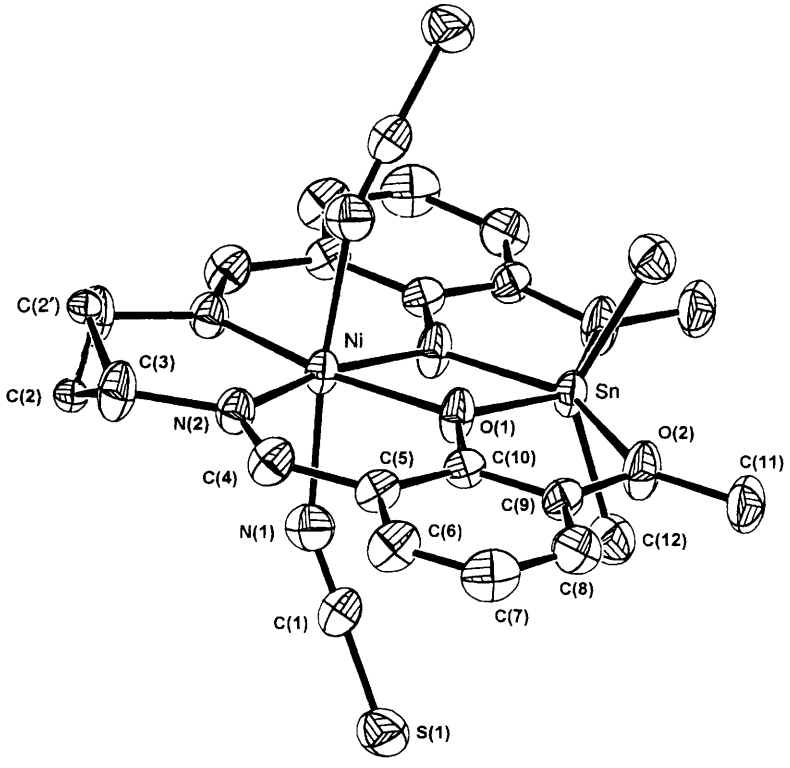

Fig. 1 The asymmetric unit of $[SnMe_2]^{2+}\cdot[Ni(3MeO\text{-}salpd)(NCS)_2]^{2-}$ **A**; C(2) and C(2') are 50% occupancy positions

The structure of Fig. 4(*a*) is a logical representation which has many parallels in organotin(IV) chemistry. For example, a number of dimethyltin(IV) cationic adducts are known [14] and, in particular, in the presence of multidentate ligands, dimethyltin dichloride has a tendency to become cationic, through loss of chloride, as has been demonstrated crystallographically in the structure of $[SnMe_2Cl(terpy)]^+[SnMe_2Cl_3]^-$ (terpy = 2,2':6',2''-terpyridine) [15] and, more relevantly, in $[SnMe_2L][PF_6]Cl$ [L = 6,6''-bis(α-methylhydrazino)-4'-phenyl-2,2':6',2''-terpyridine].[16] The structure of Fig. 4(*b*) represents the Schiff-base ligand forming a covalent complex with dimethyltin with the latter residing in the outer co-ordination site of the ligand while the inner site is occupied by the neutral molecule $Ni(NCS)_2$, similar to the manner in which, for example, $NiCl_2$ is held by the cyclam ligand (1,4,8,11-tetraazacyclotetradecane).[17] The justification for this latter structural representation rests with the very short bonds from tin to the phenolic oxygens. However, these bonds must be considered in the light of an important facet of structural tin chemistry.

Kepert [18] has conclusively shown that the co-ordination geometry for the metal M in complexes *trans*-$[ML_2X_2]$, where L and X are bidentate and monodentate ligands respectively, should have regular octahedral geometry only when L is a symmetric bidentate donor ligand and having a bite angle within a specified range. Otherwise electrostatic repulsions between bonding electron-pairs are minimised in a skew trapezoidal bipyramidal geometry and within the trapezium plane the metal makes two short and two long bonds to the

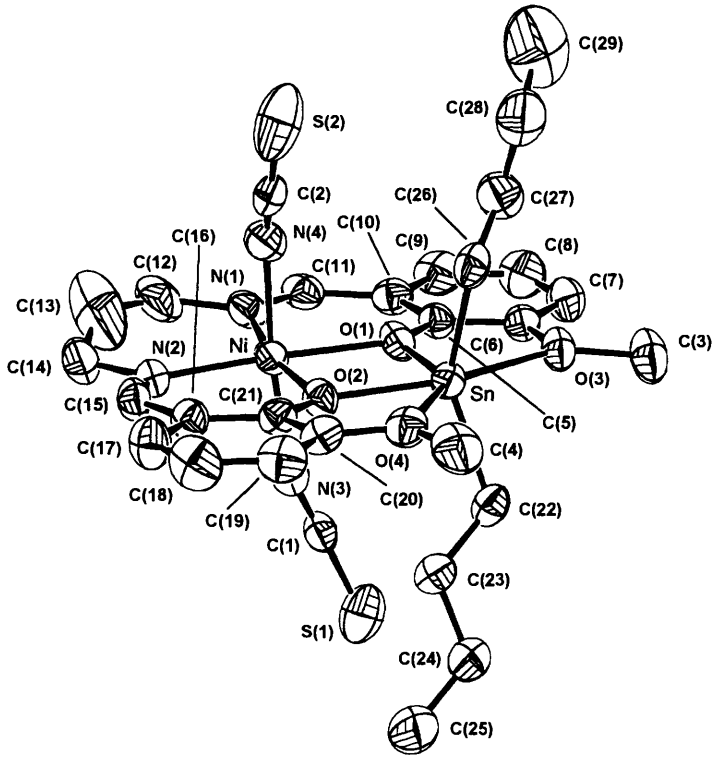

Fig. 2 The asymmetric unit of $[SnBu^n_2]^{2+}\cdot[Ni(3MeO\text{-}salpd)(NCS)_2]^{2-}$ **B**

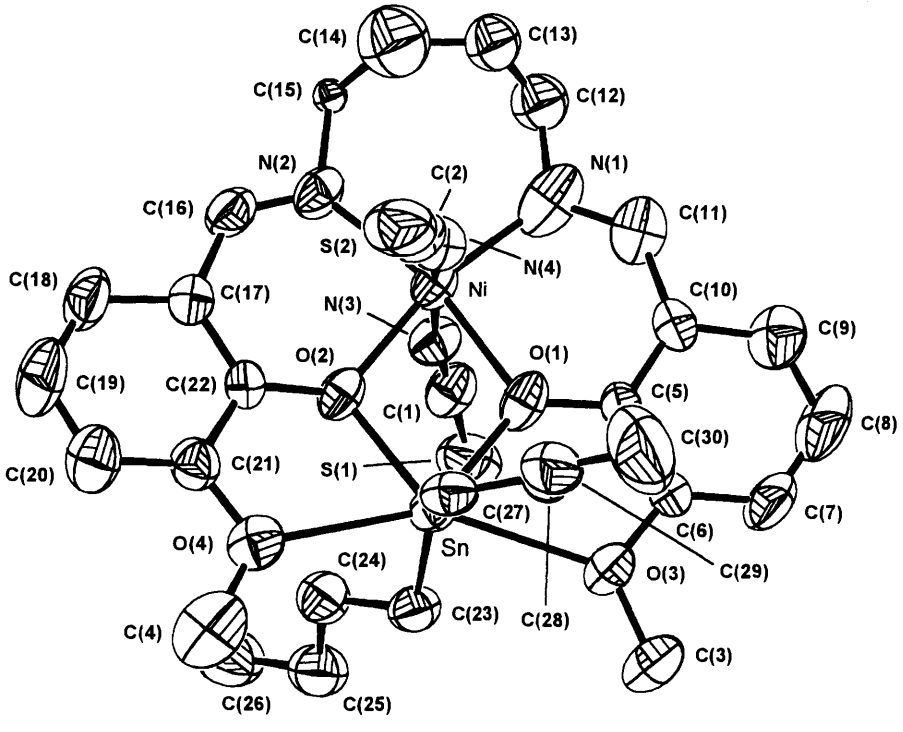

Fig. 3 The asymmetric unit of $[SnBu^n_2]^{2+}\cdot[Ni(3MeO\text{-}salbn)(NCS)_2]^{2-}$ **C**

bidentate ligand donor atoms. In complex **A** the trapezium arrangement of oxygen atoms is imposed by ligand contraints and thus, pursuing the lines of argument presented by Kepert, tin is forced to make two short and two long donor bonds in order to minimise bonding electron-pair electrostatic interactions, while, for the same reason, the axial alkyl groups are forced away from the true *trans* locations in a direction away from the short bonds. In fact, the geometry about tin in complex **A** bears a remarkable resemblance to that in $SnMe_2(O_2CMe)_2$ [19] (in this case the skew trapezoidal bipyramidal geometry results from the bite angle of the acetate ligand). In particular, the two short Sn–O bond lengths of 2.069(3) Å and the two long Sn–O bond lengths of 2.554(3) Å for **A** compare with respective lengths of 2.106(2) and 2.539(2) Å for the acetate, while the C–Sn–C bond angle of 135.3(3)° in **A** is almost identical to the analogous angle of 135.9(2)° in the acetate. Actually, it could be considered that, in **A**, two bidentate ligands, each containing a methoxy and phenolic oxygen, are complexing to tin. Since

Table 6 Fractional atomic coordinates ($\times 10^4$) for complex **D**

Atom	*x*	*y*	*z*	Atom	*x*	*y*	*z*
Sn	3378(1)	3752(1)	981(1)	C(8)	5553(3)	1208(3)	−485(2)
Ni	2196(1)	1900(1)	−184(1)	C(9)	4587(3)	1393(3)	−349(2)
S(1)	1838(2)	4100(1)	−2251(1)	C(10)	4528(2)	2146(2)	190(2)
S(2)	2615(1)	−808(1)	1680(1)	C(11)	3730(3)	767(3)	−774(2)
O(1)	1906(2)	3159(2)	442(1)	C(12)	2085(3)	61(4)	−1246(2)
O(2)	3632(2)	2401(2)	343(1)	C(13A)	997(5)	554(7)	−1531(3)
O(3)	1883(2)	4879(2)	1247(1)	C(13B)	1191(9)	−90(13)	−1131(9)
O(4)	5275(2)	3318(2)	1103(1)	C(14)	353(3)	669(4)	−1050(3)
O(5)	4322(2)	5355(3)	1880(2)	C(15)	−30(3)	2049(3)	−315(2)
N(1)	2177(3)	3094(3)	−960(2)	C(16)	72(2)	2942(3)	188(2)
N(2)	2244(2)	726(3)	600(2)	C(17)	−856(3)	3329(3)	326(2)
N(3)	2794(2)	803(3)	−765(1)	C(18)	−874(3)	4206(4)	769(2)
N(4)	681(2)	1571(3)	−538(2)	C(19)	25(3)	4749(3)	1092(2)
N(5)	4966(3)	7001(3)	2371(2)	C(20)	936(2)	4390(3)	968(2)
C(1)	2045(3)	3504(3)	−1499(2)	C(21)	981(2)	3479(3)	527(2)
C(2)	2395(2)	101(3)	1050(2)	C(22)	3528(3)	2910(3)	1925(2)
C(3)	1901(3)	5891(3)	1624(2)	C(23)	3562(3)	5061(3)	316(2)
C(4)	6157(3)	3678(4)	1603(2)	C(24)	4876(4)	6174(4)	1919(2)
C(5)	5426(2)	2625(2)	585(2)	C(25)	4319(3)	7016(4)	2860(2)
C(6)	6369(2)	2411(3)	446(2)	C(26)	5636(5)	7939(5)	2387(3)
C(7)	6419(3)	1707(3)	−99(2)				

Table 7 Fractional atomic coordinates ($\times 10^4$) for complex **E**

Atom	*x*	*y*	*z*	Atom	*x*	*y*	*z*
Sn	2112(1)	698(1)	2894(1)	C(13A)	2550(10)	5402(8)	877(4)
Ni	2137(1)	3100(1)	1868(1)	C(13B)	1561(12)	5375(10)	1024(5)
S(1)	6653(1)	3546(1)	845(1)	C(14)	1107(6)	4114(5)	585(2)
S(2)	2022(2)	−3575(1)	3914(1)	C(15)	−241(4)	1724(4)	600(2)
O(1)	3133(2)	2911(2)	2821(1)	C(16)	−771(4)	354(4)	810(2)
O(2)	1030(2)	1012(2)	1912(1)	C(17)	−2024(4)	−736(4)	352(2)
O(3)	4265(3)	2154(2)	3910(1)	C(18)	−2629(5)	−2063(4)	485(2)
O(4)	−91(3)	−1538(2)	2179(1)	C(19)	−2012(4)	−2394(4)	1091(2)
N(1)	2200(4)	−1037(4)	3584(2)	C(20)	−786(4)	−1331(3)	1554(2)
N(2)	3966(4)	2998(3)	1420(2)	C(21)	−150(4)	40(3)	1433(2)
N(3)	212(4)	3329(3)	2293(2)	C(22)	4528(6)	1817(5)	4592(2)
N(4)	3310(4)	5206(3)	2076(2)	C(23)	−678(6)	−2941(4)	2314(3)
N(5)	842(3)	2877(3)	922(2)	C(24)	3763(4)	199(3)	2415(2)
C(1)	−816(5)	3453(4)	2484(2)	C(25)	5035(4)	126(4)	2819(2)
C(2)	−2116(5)	3603(5)	2748(2)	C(26)	6166(5)	−104(4)	2510(3)
C(3)	2156(4)	−2080(4)	3726(2)	C(27)	6036(5)	−269(4)	1796(3)
C(4)	5082(4)	3227(4)	1181(2)	C(28)	4759(5)	−241(1)	1384(2)
C(5)	4381(4)	3913(3)	3249(2)	C(29)	3634(4)	5(4)	1696(2)
C(6)	5038(4)	3543(4)	3837(2)	C(30)	590(4)	964(3)	3561(2)
C(7)	6343(5)	4508(4)	4300(2)	C(31)	673(4)	2287(4)	3778(2)
C(8)	6994(5)	5883(5)	4182(2)	C(32)	−240(5)	2487(4)	4244(2)
C(9)	6359(5)	6260(4)	3624(2)	C(33)	−1235(5)	1379(5)	4500(2)
C(10)	5036(4)	5302(4)	3144(2)	C(34)	−1328(5)	62(5)	4285(2)
C(11)	4425(5)	5863(4)	2589(2)	C(35)	−423(4)	−153(4)	3823(2)
C(12)	2954(7)	6034(5)	1580(3)				

Table 8 Selected bond lengths (Å) and angles (°) for complex **A**

Sn–O(1)	2.069(3)	Ni–N(2)	2.005(3)
Ni–N(1)	2.095(4)	N(1)–C(1)	1.148(6)
S(1)–C(1)	1.633(5)	Sn–C(12)	2.096(4)
Sn–O(2)	2.554(3)	Ni–O(1)	2.057(3)
O(1′)–Sn–O(1)	75.4(2)	O(1′)–Sn–C(12)	106.1(2)
O(1)–Sn–C(12)	108.9(2)	C(12)–Sn–C(12′)	135.3(3)
C(12)–Sn–O(2′)	84.9(2)	O(1)–Sn–O(2)	67.19(10)
C(12)–Sn–O(2)	83.9(2)	O(2′)–Sn–O(2)	150.31(14)
N(2′)–Ni–N(2)	101.2(2)	N(2)–Ni–O(1)	91.53(13)
O(1′)–Ni–O(1)	75.9(2)	N(2′)–Ni–N(1)	96.1(2)
N(2)–Ni–N(1)	87.81(14)	O(1′)–Ni–N(1)	88.36(14)
O(1)–Ni–N(1)	86.8(2)	N(1)–Ni–N(1′)	173.9(2)

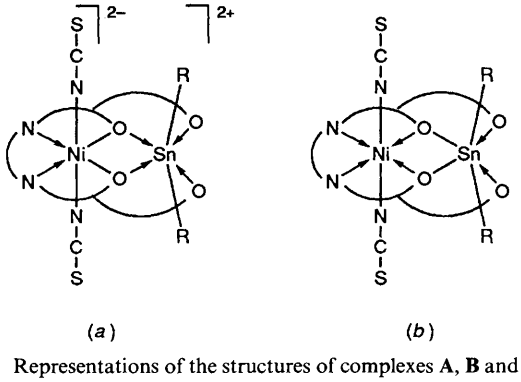

Fig. 4 Representations of the structures of complexes **A**, **B** and **C**

these are unsymmetrical ligand moieties it is probably the case, viewed in terms of Kepert's arguments, that the geometry about tin is not particularly different to that which would be observed if the two ligand moieties could behave independently of each other. The important conclusion to be drawn from the above arguments is that the unexpectedly short Sn–O bonds to the

Table 9 Selected bond lengths (Å) and angles (°) for complex **B**

Sn–O(1)	2.095(3)	Ni–N(2)	2.017(4)
Sn–O(4)	2.567(4)	Ni–N(3)	2.067(5)
Ni–N(1)	2.008(4)	N(3)–C(1)	1.153(7)
Ni–O(2)	2.058(3)	Sn–O(3)	2.603(3)
S(1)–C(1)	1.622(6)	Sn–C(26)	2.106(5)
N(4)–C(2)	1.109(7)	Ni–O(1)	2.060(3)
Sn–O(2)	2.088(3)	Ni–N(4)	2.089(5)
Sn–C(22)	2.126(5)	S(2)–C(2)	1.626(6)
O(2)–Sn–O(1)	74.87(12)	O(2)–Sn–C(26)	105.2(2)
O(1)–Sn–C(26)	101.1(2)	O(2)–Sn–C(22)	101.8(2)
O(1)–Sn–C(22)	105.7(2)	C(26)–Sn–C(22)	145.9(2)
O(2)–Sn–O(4)	67.29(12)	C(26)–Sn–O(4)	83.9(2)
C(22)–Sn–O(4)	87.8(2)	O(1)–Sn–O(3)	66.54(11)
C(26)–Sn–O(3)	90.7(2)	C(22)–Sn–O(3)	81.2(2)
O(4)–Sn–O(3)	151.73(11)	N(1)–Ni–N(2)	99.4(2)
N(2)–Ni–O(2)	92.1(2)	N(1)–Ni–O(1)	92.2(2)
O(2)–Ni–O(1)	76.24(13)	N(1)–Ni–N(3)	90.3(2)
N(2)–Ni–N(3)	96.2(2)	O(2)–Ni–N(3)	90.4(2)
O(1)–Ni–N(3)	85.8(2)	N(1)–Ni–N(4)	93.0(2)
N(2)–Ni–N(4)	88.4(2)	O(2)–Ni–N(4)	85.3(2)
O(1)–Ni–N(4)	88.8(2)	N(3)–Ni–N(4)	173.8(2)
C(1)–N(3)–Ni	162.3(4)	C(2)–N(4)–Ni	157.2(5)
N(3)–C(1)–S(1)	178.0(5)	N(4)–C(2)–S(2)	175.0(6)

Table 10 Selected bond lengths (Å) and angles (°) for complex **C**

Sn–O(1)	2.082(4)	Ni–N(2)	2.048(6)
Sn–O(4)	2.545(5)	Ni–O(1)	2.091(4)
Ni–N(1)	2.037(6)	N(3)–C(1)	1.145(9)
Ni–N(4)	2.057(8)	Sn–O(3)	2.581(5)
S(1)–C(1)	1.627(9)	Sn–C(27)	2.124(7)
N(4)–C(2)	1.128(10)	Ni–N(3)	2.056(7)
Sn–O(2)	2.096(4)	Ni–O(2)	2.083(4)
Sn–C(23)	2.116(7)	S(2)–C(2)	1.624(9)
O(1)–Sn–O(2)	75.1(2)	O(1)–Sn–C(23)	105.8(3)
O(2)–Sn–C(23)	101.7(2)	O(1)–Sn–C(27)	101.8(3)
O(2)–Sn–C(27)	105.1(2)	C(23)–Sn–C(27)	145.5(3)
O(2)–Sn–O(4)	68.4(2)	C(23)–Sn–O(4)	86.9(2)
C(27)–Sn–O(4)	83.2(2)	O(1)–Sn–O(3)	67.3(2)
C(23)–Sn–O(3)	81.5(2)	C(27)–Sn–O(3)	90.6(2)
O(4)–Sn–O(3)	149.6(2)	N(1)–Ni–N(2)	103.7(2)
N(1)–Ni–N(4)	93.2(3)	N(2)–Ni–N(4)	90.1(3)
N(1)–Ni–N(3)	89.9(3)	N(2)–Ni–N(3)	94.9(2)
N(4)–Ni–N(3)	173.3(3)	N(2)–Ni–O(2)	90.4(2)
N(4)–Ni–O(2)	84.8(2)	N(3)–Ni–O(2)	90.7(2)
N(1)–Ni–O(1)	90.6(2)	N(4)–Ni–O(1)	88.2(2)
N(3)–Ni–O(1)	85.9(2)	O(2)–Ni–O(1)	75.2(2)
C(1)–N(3)–Ni	161.9(6)	C(2)–N(4)–Ni	162.0(7)
N(3)–C(1)–S(1)	177.7(7)	N(4)–C(2)–S(2)	176.1(8)

Table 11 Selected bond lengths (Å) and angles (°) for complex **D**

Sn–O(1)	2.127(2)	S(1)–C(1)	1.618(4)
Sn–O(4)	2.548(2)	N(2)–C(2)	1.142(4)
Sn–C(23)	2.093(3)	N(5)–C(25)	1.451(6)
Ni–N(3)	2.030(3)	Sn–O(3)	2.565(2)
Ni–O(2)	2.048(2)	Sn–C(22)	2.095(3)
S(2)–C(2)	1.628(3)	Ni–N(2)	2.082(3)
N(5)–C(24)	1.318(5)	Ni–O(1)	2.041(2)
Sn–O(2)	2.124(2)	N(1)–C(1)	1.154(5)
Sn–O(5)	2.709(3)	O(5)–C(24)	1.214(5)
Ni–N(1)	2.092(3)	N(5)–C(26)	1.426(6)
Ni–N(4)	2.020(3)		
C(23)–Sn–C(22)	157.0(2)	C(23)–Sn–O(2)	96.92(13)
C(22)–Sn–O(2)	100.50(12)	C(23)–Sn–O(1)	99.28(12)
C(22)–Sn–O(1)	99.99(13)	O(2)–Sn–O(1)	73.16(8)
C(23)–Sn–O(4)	86.80(12)	C(22)–Sn–O(4)	86.48(12)
O(2)–Sn–O(4)	66.72(7)	C(23)–Sn–O(3)	87.72(12)
C(22)–Sn–O(3)	88.62(12)	O(1)–Sn–O(3)	66.50(7)
O(4)–Sn–O(3)	153.63(7)	C(23)–Sn–O(5)	77.92(13)
C(22)–Sn–O(5)	79.19(12)	O(4)–Sn–O(5)	77.38(8)
O(3)–Sn–O(5)	76.25(8)	C(24)–O(5)–Sn	141.8(3)
O(5)–C(24)–N(5)	126.4(4)	N(4)–Ni–N(3)	100.28(11)
N(4)–Ni–O(1)	91.86(10)	N(3)–Ni–O(2)	91.52(10)
O(1)–Ni–O(2)	76.56(8)	N(4)–Ni–N(2)	88.91(13)
N(3)–Ni–N(2)	93.01(12)	O(1)–Ni–N(2)	90.46(11)
O(2)–Ni–N(2)	87.33(11)	N(4)–Ni–N(1)	92.27(13)
N(3)–Ni–N(1)	87.10(12)	O(1)–Ni–N(1)	89.17(12)
O(2)–Ni–N(1)	91.45(12)	N(2)–Ni–N(1)	178.78(13)
C(1)–N(1)–Ni	161.0(3)	C(2)–N(2)–Ni	171.8(3)
N(1)–C(1)–S(1)	178.6(3)	N(2)–C(2)–S(2)	178.9(3)

phenolic oxygens almost certainly arise from the minimisation of electrostatic interactions between bonding electron-pairs and consequently the most reasonable representation of the structures of complexes **A**, **B** and **C** is that of Fig. 4(*a*). They thus represent an interesting class of zwitterionic, or intimate ion-paired, heterobimetallic complexes. It is also noteworthy that **B** and **C** present the first crystallographic evidence for the existence of the dibutyltin cation $[SnBu^n_2]^{2+}$.

Reference to Figs. 1–3 and to the bond angle data of Tables 8–10 reveals that there is a considerable volume of the tin co-ordination sphere which is unoccupied in each of the complexes **A**, **B** and **C**. As a result, tin readily forms another donor bond thus expanding its co-ordination number to seven. For example, this paper includes dmf adducts of each of the complexes and in the case of **B** and **C** the tendency for donor-bond formation is further seen in the molecular association which occurs in their crystal structures. Strikingly similar molecular alignment occurs in the crystal structures of complexes **B** and **C** (see Fig. 5) whereby, in each case, a thiocyanate sulfur sits close to the least-squares plane defined by the Schiff-base oxygens and tin of a neighbouring molecule. It is almost equidistant from the methoxy oxygens while it is 3.747 Å away from tin in **B** and 3.808 Å in **C**. The tin co-ordination geometry in both **B** and **C** can be described as pseudo-pentagonal bipyramidal. While the intermolecular Sn–S bond lengths are close to the sum of the van der Waals radii for tin and sulfur, they do have a significant influence on the immediate tin co-ordination geometry, particularly on the C–Sn–C bond angles. For example, the C–Sn–C bond angle of 135.3(3)° in **A** (which does not have an intermolecular Sn–S bond) compares with analogous values of 145.9(2)° in **B** and 145.5(3)° in **C**. The intermolecular interaction also has the effect of withdrawing tin very slightly from the phenolic oxygen atoms such that the Sn–O bond lengths (involving the phenolic oxygens) increase, on average, by approximately 0.02 Å.

The adduct $[SnMe_2{\cdot}dmf]^{2+}{\cdot}[Ni(3MeO\text{-}salpd)]^{2-}$ **D** contains tin in a pentagonal bipyramidal co-ordination environment with the Schiff-base and dmf oxygens in the equatorial plane and the methyl groups axial. Dimethylformamide forms a relatively weak donor bond to tin (see Fig. 6 and Table 11). For example, the Sn–dmf donor-bond length of 2.709(3) Å in **D** compares with analogous bond lengths of 2.39(2) Å for $SnMe_2Cl_2{\cdot}2dmf$,[20] 2.22(2) Å for $SnMeCl_3{\cdot}2dmf$,[21] and 2.194(6) and 2.209(6) Å for $SnBu^nCl_3{\cdot}2dmf$.[22] This is also reflected in the infrared carbonyl stretching frequency data. For example, for unco-ordinated dmf this frequency occurs at 1684 cm^{-1} whereas for $SnCl_4{\cdot}2dmf$, $SnBu^nCl_3{\cdot}2dmf$ and **D**, it occurs at 1612, 1642 and 1660 cm^{-1} respectively. Although the dmf donor bond is relatively weak, it is considerably stronger than the intermolecular Sn–S bonds in **B** and **C**, and consequently the C–Sn–C angle which is 135.3(3)° in **A** and approximately 146° in both **B** and **C** (as a result of the Sn–S intermolecular contacts) is further increased to 157.0(2)° in **D**. A further effect of the dmf interaction is to increase the Sn–O bond lengths, involving the phenolic oxygens, from 2.069(3) Å in **A** to values of 2.124(2) and 2.127(2) Å in **D**. Furthermore, the Sn–Ni separation of 3.259 Å in **A** compares with a separation of 3.311 Å in **D**.

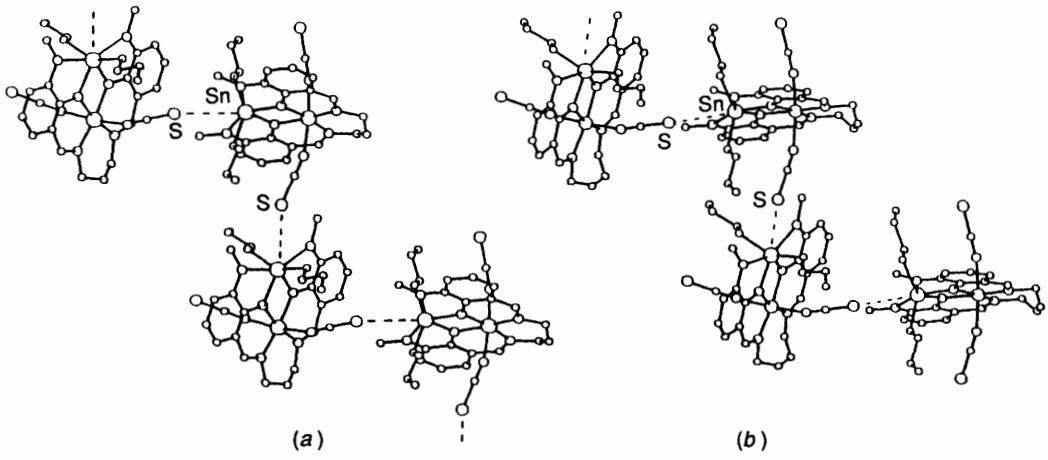

Fig. 5 Intermolecular Sn–S bonding (dashed lines) in (*a*) complex **B** and (*b*) complex **C**

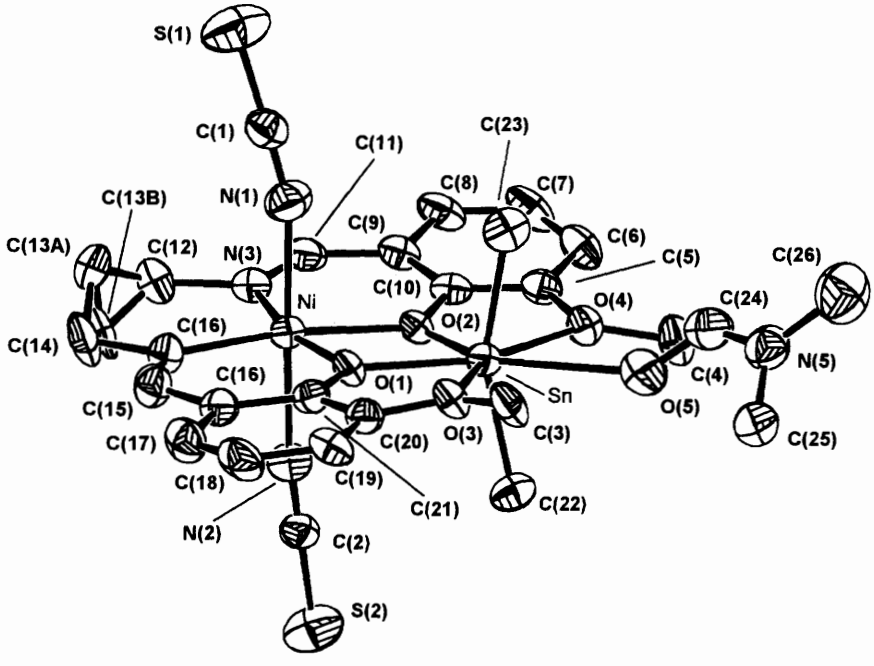

Fig. 6 The asymmetric unit of $[SnMe_2 \cdot dmf]^{2+} \cdot [Ni(3MeO\text{-}salpd)(NCS)_2]^{2-}$ **D**; C(13A) and C(13B) are 50% occupancy sites

The significant difference between the reactions of dialkyltin(IV) diisothiocyanates and diphenyltin diisothiocyanate with $[Ni(3MeO\text{-}salpd)] \cdot H_2O$ is that in the latter only one thiocyanate group migrates from tin thus yielding the complex $[SnPh_2(NCS)]^+ \cdot [Ni(3MeO\text{-}salpd)(NCS)(MeCN)]^-$ **E**. In general, we have found that the reactions of $SnPh_2X_2$ (X = halide, thiocyanate or nitrate) with [M(3MeO-salpd)] (M = Ni, Cu or Co) lead to the transfer of only one group X from tin and this may suggest a general reluctance for the formation of the diphenyltin cation $[SnPh_2]^{2+}$. The geometry about tin in **E** (see Fig. 7 and Table 12) is similar to that about tin in **D**. In complex **E** the Schiff-base oxygens and N(1) (*i.e.* the nitrogen of the thiocyanate group bonded to tin) define the equatorial plane, and these atoms and tin are essentially coplanar. The Sn–N donor bond length of 2.408(3) Å in **E** is significantly shorter than the Sn–O (where O is the dmf donor oxygen) donor bond length of 2.709(3) Å in **D** and thus the C–Sn–C bond angle of 157.0(2)° in the latter is increased to 166.74(12)° in **E**. Furthermore, the average distance from tin to the phenolic oxygens in **D** [2.107(9) Å] increases significantly to 2.179(4) Å in **E**. This is accompanied by an increase in the Sn–Ni distance from 3.311 Å in **D** to 3.387 Å in **E**. Thus, in general terms as the donor bond to tin *trans* to the phenolic oxygens increases in strength there is a progressive increase in the C–Sn–C bond angle, the tin–phenolic oxygen bond lengths and the Sn–Ni separation.

The same Schiff-base ligand is complexed to nickel in complexes **A**, **B** and **D**, and in each case octahedral geometry is completed by *trans* thiocyanate groups. Bond lengths and angles are in no way abnormal, the only noteworthy feature being that **D** has the shortest Ni–O and the longest Ni–N bonds of the three. This appears to be a consequence of **D** having the weakest tin–phenolic oxygen bonds. Complexes **B** and **C** differ only in that the latter has an extra carbon in the imine nitrogen bridge. The longer bridge results in the average Ni–O and Ni–N bond lengths increasing by 0.028 and 0.03 Å respectively.

The Sn-119 Mössbauer and selected infrared data of Table 13 are readily interpreted in terms of the crystallographic data, and furthermore provide valuable structural information regarding the zinc and copper complexes which could not be crystallised. In all of the complexes of Table 13 the shifts in the phenolic ν(C–O) stretching frequencies which occur on adduct formation are generally greater than those observed when adducts are formed in the absence of the methoxy substituents[4] and this is

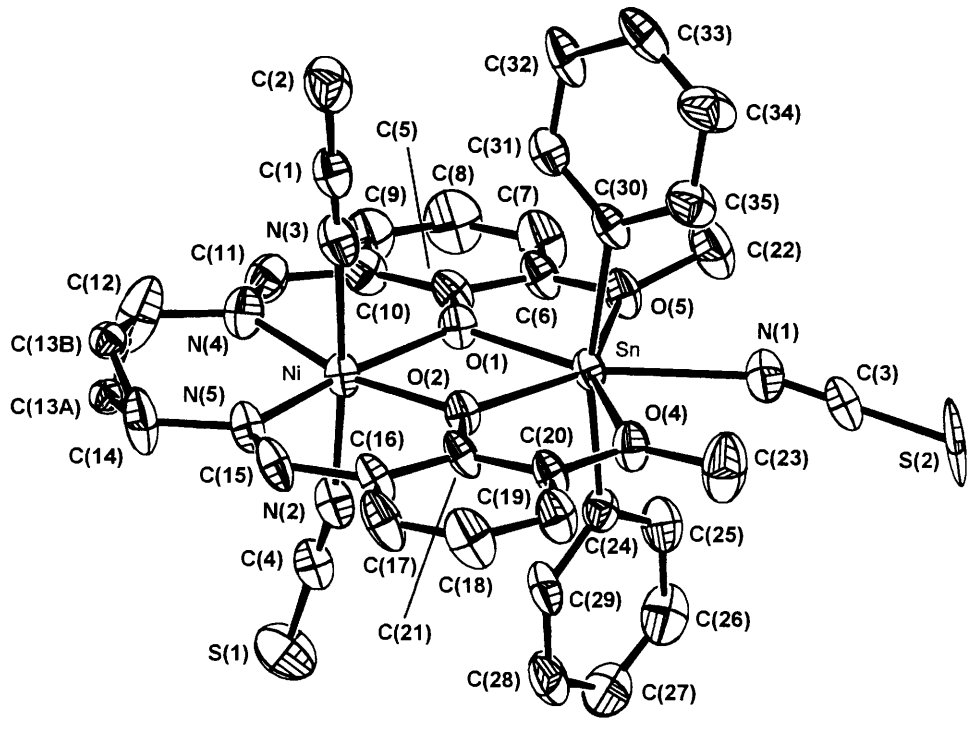

Fig. 7 The asymmetric unit of $[SnPh_2(NCS)]^+ \cdot [Ni(3MeO\text{-}salpd)(NCS)(MeCN)]^-$ **E**; C(13A) and C(13B) are 50% occupancy sites

Table 12 Selected bond lengths (Å) and angles (°) for complex **E**

Sn–O(1)	2.172(2)	Ni–N(3)	2.175(3)
Sn–O(4)	2.557(2)	N(1)–C(3)	1.149(5)
Sn–C(30)	2.132(3)	C(1)–C(2)	1.447(5)
Ni–N(2)	2.066(3)	Sn–O(3)	2.512(2)
Ni–N(5)	2.023(3)	Sn–C(24)	2.120(3)
N(3)–C(1)	1.132(4)	Ni–O(2)	2.046(2)
S(1)–C(4)	1.625(4)	Ni–N(4)	2.018(3)
Sn–O(2)	2.182(2)	S(2)–C(3)	1.618(4)
Sn–N(1)	2.408(3)	N(2)–C(4)	1.153(4)
Ni–O(1)	2.046(2)		
C(24)–Sn–C(30)	166.74(12)	C(24)–Sn–O(1)	96.00(11)
C(30)–Sn–O(1)	92.25(11)	C(24)–Sn–O(2)	92.82(11)
C(30)–Sn–O(2)	99.71(10)	O(1)–Sn–O(2)	70.63(8)
C(24)–Sn–N(1)	82.77(12)	C(30)–Sn–N(1)	84.51(12)
C(24)–Sn–O(3)	88.86(11)	C(30)–Sn–O(3)	84.80(10)
O(1)–Sn–O(3)	67.11(8)	N(1)–Sn–O(3)	77.90(10)
C(24)–Sn–O(4)	89.53(11)	C(30)–Sn–O(4)	91.56(10)
O(2)–Sn–O(4)	66.25(8)	O(3)–Sn–O(4)	156.11(8)
N(1)–Sn–O(4)	78.25(10)	C(3)–N(1)–Sn	160.5(3)
N(1)–C(3)–S(2)	177.8(4)	N(4)–Ni–N(5)	99.69(13)
N(5)–Ni–O(2)	92.50(11)	N(4)–Ni–O(1)	91.65(11)
O(2)–Ni–O(1)	75.91(8)	N(4)–Ni–N(2)	88.83(13)
N(5)–Ni–N(2)	92.07(12)	O(2)–Ni–N(2)	96.86(11)
O(1)–Ni–N(2)	91.16(10)	N(4)–Ni–N(3)	88.29(12)
N(5)–Ni–N(3)	85.14(12)	O(2)–Ni–N(3)	86.67(10)
O(1)–Ni–N(3)	92.24(10)	N(2)–Ni–N(3)	175.61(12)
C(4)–N(2)–Ni	166.3(3)	N(2)–C(4)–S(1)	179.9(4)
C(1)–N(3)–Ni	176.9(3)	N(3)–C(1)–C(2)	178.3(4)

consistent with the very strong Sn–O donor bonds which have been observed in the present study. The two thiocyanate groups in complex **A** are related by the crystallographic two-fold axis and thus only one thiocyanate ν(C–N) stretching frequency (2086 cm^{-1}) is observed. Since only one thiocyanate ν(C–N) stretching frequency (2085 cm^{-1}) is observed for $[SnMe_2]^{2+} \cdot [Ni(3MeO\text{-}salbn)(NCS)_2]^{2-}$ clearly the two thiocyanate groups are also in similar environments. By contrast, the weak bridging role adopted by one thiocyanate ligand in both **B** and **C** results in two closely spaced thiocyanate stretching frequencies in their infrared spectra. However, when these complexes form dmf adducts, the thiocyanate bridging role no longer exists and consequently only one thiocyanate stretching frequency is observed. In **E** the thiocyanate stretching frequency at 2094 cm^{-1} is clearly associated with the thiocyanate co-ordinated to nickel, while the band at a considerably lower frequency (2049 cm^{-1}) is attributed to the thiocyanate which is co-ordinated to tin.

Complex **A** is the only tin–nickel complex which has tin in a six-co-ordinated environment and its skew trapezoidal geometry gives rise to a C–Sn–C bond angle of 135.3(3)°. All other tin–nickel complexes have tin either in pseudo-pentagonal bipyramidal or true pentagonal bipyramidal co-ordination environments as a result of which the C–Sn–C bond angles are always greater than that of **A**. Predictably therefore, **A** exhibits the smallest Mössbauer quadrupole splitting of 3.60 mm s^{-1}. The progressive increase in C–Sn–C bond angles from **A** to **B** (and **C**) to **D** is marked by a progressive and decisive increase in quadrupole splitting to a value of 4.45 mm s^{-1} in **D**. In the light of these trends it is not surprising that the formation of a dmf adduct always results in a substantial increase in quadrupole splitting. The large quadrupole splitting for **E** [it should be borne in mind that the quadrupole splitting of a diphenyltin(IV) complex will be smaller than that of a dimethyl- or dibutyltin(IV) analogue] is also consistent with its large C–Sn–C bond angle.

That the zinc and copper complexes, excluding the complex having Cu(3MeO-salbn) as the Schiff-base derivative, are correctly formulated as $[SnR_2(NCS)]^+ \cdot [M(L)(NCS)]^- \cdot nH_2O$ (R = Me or Bu^n; M = Cu or Zn; L = Schiff-base ligand; n = 0, 1 or 2) is clearly evident from infrared and Mössbauer spectroscopic data. They all exhibit two thiocyanate related ν(C–N) stretching frequencies in their infrared spectra, one of which lies in the range 2034–2045 cm^{-1}, and by analogy with the data for the nickel–tin complexes this band is almost certainly associated with a thiocyanate co-ordinated to tin. Their Mössbauer quadrupole splittings are extremely large and, bearing in mind the analysis of the quadrupole splitting data for the tin–nickel complexes, point to seven-co-ordinated tin environments. The complex containing Cu(3MeO-salbn) as the Schiff-base derivative is exceptional among the tin–copper complexes as it does not contain a ν(C–N) stretching frequency

Table 13 Tin-119 Mössbauer and selected infrared spectroscopic data for the complexes[a]

Complex	δ/mm s^{-1}	Δ/mm s^{-1}	ν̃(C–O)[b]/cm^{-1}	ν̃(C–N)/cm^{-1}
$[SnMe_2]^{2+}\cdot[Ni(3MeO\text{-}salpd)(NCS)_2]^{2-}$	1.21	3.60	1565	2086
$[SnMe_2\cdot dmf]^{2+}\cdot[Ni(3MeO\text{-}salpd)(NCS)_2]^{2-}$	1.43	4.45	1660 1565	2080
$[SnBu^n_2]^{2+}\cdot[Ni(3MeO\text{-}salpd)(NCS)_2]^{2-}$	1.55	4.05	1567	2094 2086
$[SnBu^n_2\cdot dmf]^{2+}\cdot[Ni(3MeO\text{-}salpd)(NCS)_2]^{2-}$	1.64	4.38	1660 1565	2080
$[SnMe_2]^{2+}\cdot[Ni(3MeO\text{-}salbn)(NCS)_2]^{2-}$	1.35	3.90	1570	2085
$[SnMe_2\cdot dmf]^{2+}\cdot[Ni(3MeO\text{-}salbn)(NCS)_2]^{2-}$	1.49	4.49	1660 1571	2084
$[SnBu^n_2]^{2+}\cdot[Ni(3MeO\text{-}salbn)(NCS)_2]^{2-}$	1.50	3.89	1568	2093 2083
$[SnBu^n_2\cdot dmf]^{2+}\cdot[Ni(3MeO\text{-}salbn)(NCS)_2]^{2-}$	1.55	4.15	1660 1569	2084
$[SnPh_2(NCS)]^{+}\cdot[Ni(3MeO\text{-}salpd)(NCS)(MeCN)]^{-}$	1.19	4.31	1570	2094 2049
$[SnMe_2(NCS)]^{+}\cdot[Cu(3MeO\text{-}salpd)(NCS)]^{-}$	1.44	4.87	1567	2057 2034
$[SnMe_2(NCS)]^{+}\cdot[Cu(3MeO\text{-}salpd)(NCS)]^{-}\cdot 2H_2O$	1.46	4.86	1570	2062 2045
$[SnBu^n_2(NCS)]^{+}\cdot[Cu(3MeO\text{-}salpd)(NCS)]^{-}\cdot H_2O$	1.63	4.80	1565 1550	2064 2043
$[SnMe_2]^{2+}\cdot[Cu(3MeO\text{-}salbn)(NCS)_2]^{2-}\cdot H_2O$	1.21	3.82	1550	2088 2072
$[SnBu^n_2(NCS)]^{+}\cdot[Zn(3MeO\text{-}salpd)(NCS)]^{-}$	1.58	4.62	1560	2084 2043

[a] All Mössbauer data are ± 0.02 mm s^{-1}; ν(C–O) for $[Ni(3MeO\text{-}salpd)]\cdot H_2O$, $[Ni(3MeO\text{-}salbn)]\cdot H_2O$, [Cu(3MeO-salpd)] and [Zn(3MeO-salpd)] occur at 1545, 1549, 1541 and 1548 cm^{-1} respectively. [b] The band at 1660 cm^{-1} is, in all cases, associated with the dimethylformamide ligand.

below 2045 cm^{-1} and its quadrupole splitting is very significantly smaller than those observed for the other complexes. The two observed ν(C–N) stretching frequencies at 2088 and 2072 cm^{-1} coupled with the quadrupole splitting of 3.82 mm s^{-1} point to a complex containing the $[SnMe_2]^{2+}$ cation in an associated structure similar to that of **C**.

The complexes $[SnMe_2(NCS)]^{+}\cdot[Cu(3MeO\text{-}salpd)(NCS)]^{-}$ and $[SnBu^n_2(NCS)]^{+}\cdot[Zn(3MeO\text{-}salpd)(NCS)]^{-}$ clearly contain five-co-ordinated copper and zinc respectively. The co-ordination geometry about the metal in each case is probably similar to the approximately square-pyramidal geometry which we observed about the zinc and nickel atoms co-ordinated directly to the Schiff-base ligand in $Zn[Zn(3MeO\text{-}salpd)(NCS)]_2$ and $Ni[Ni(3MeO\text{-}salbn)(NCS)]_2$ respectively.[22,23] For the two remaining complexes of Table 13 containing Cu(3MeO-salpd), copper may have octahedral geometry as a result of co-ordinated water.

Acknowledgements

J. McG. is grateful to the Higher Education Authority of Ireland for financial support.

References

1 M. D. Hobday and T. D. Smith, *J. Chem. Soc. A*, 1971, 1453.
2 L. Pellerito, R. Cefalu, A. Gianguzza and R. Barbieri, *J. Organomet. Chem.*, 1974, **70**, 303.
3 T. N. Strivastava, A. K. S. Chauhan and M. Agarwal, *Transition Met. Chem.*, 1978, **3**, 378.
4 D. Cunningham, J. Fitzgerald and M. Little, *J. Chem. Soc., Dalton Trans.*, 1987, 2261.
5 D. Cunningham and J. McGinley, *J. Chem. Soc., Dalton Trans.*, 1992, 1387.
6 D. Cunningham, J. F. Gallagher, T. Higgins, P. McArdle, J. McGinley and M. O'Gara, *J. Chem. Soc., Dalton Trans.*, 1993, 2183.
7 N. Clarke, D. Cunningham, T. Higgins, P. McArdle, J. McGinley and M. O'Gara, *J. Organomet. Chem.*, 1994, **469**, 33.
8 M. Calligaris, L. Randaccio, R. Barbieri and L. Pellerito, *J. Organomet. Chem.*, 1974, **76**, C56.
9 D. Cunningham, T. Higgins, B. Kneafsey, P. McArdle and J. Simmie, *J. Chem. Soc., Chem. Commun.*, 1985, 231.
10 G. M. Sheldrick, SHELX 86, a computer program for crystal structure determination, University of Göttingen, 1986.
11 G. M. Sheldrick, SHELX 93, a computer program for crystal structure determination, University of Göttingen, 1993.
12 C. K. Johnson, ORTEP, Report ORNL (US), revised, Oak Ridge National Laboratory, Oak Ridge, TN, 1971, pp. 1965–3794.
13 D. S. Motherwell, PLUTO, Cambridge University, 1974.
14 V. G. Kumar Das and W. Kitching, *J. Organomet. Chem.*, 1967, **10**, 59.
15 F. W. B. Einstein and B. R. Penfold, *J. Chem. Soc. A*, 1968, 3019.
16 E. C. Constable, F. K. Khan, J. Lewis, M. C. Liptrot and P. R. Raithby, *J. Chem. Soc., Dalton Trans.*, 1985, 333.
17 B. Bosnich, R. Mason, P. Pauling, G. B. Robertson and M. L. Tobe, *Chem. Commun.*, 1965, 97.
18 D. L. Kepert, *J. Organomet. Chem.*, 1976, **107**, 49.
19 T. P. Lockhart, J. C. Calabrese and F. Davidson, *Organometallics*, 1987, **6**, 2479.
20 L. A. Aslanov, V. M. Ionov, W. M. Attia, A. B. Permin and V. S. Petrosyan, *J. Organomet. Chem.*, 1978, **144**, 39.
21 L. A. Aslanov, V. M. Ionov, W. M. Attia, A. B. Perkin and V. S. Petrosyan, *Zn. Strukt. Khim.*, 1978, **19**, 315.
22 J. McGinley, Ph.D. Thesis, National University of Ireland, 1990.
23 D. Sheerin, Ph.D. Thesis, National University of Ireland, 1991.

Received 21*st March* 1994; *Paper* 4/01668H